Bioorganic & Medicinal Chemistry 16 (2008) 7777–7787

Contents lists available at ScienceDirect

Bioorganic & Medicinal Chemistry

journal homepage: www.elsevier.com/locate/bmc

Novel dimeric aryldiketo containing inhibitors of HIV-1 integrase: Effects of the phenyl substituent and the linker orientation

Li-Fan Zeng [a], Xiao-Hua Jiang [a], Tino Sanchez [b], Hu-Shan Zhang [a], Raveendra Dayam [b], Nouri Neamati [b,*], Ya-Qiu Long [a,*]

[a] State Key Laboratory of Drug Research, Shanghai Institute of Materia Medica, Shanghai Institutes for Biological Sciences, Chinese Academy of Sciences, 555 Zuchongzhi Road, Shanghai 201203, China

[b] Department of Pharmacology and Pharmaceutical Sciences, School of Pharmacy, University of Southern California, 1985 Zonal Avenue, Los Angeles, CA 90089, United States

ARTICLE INFO

Article history:
Received 29 May 2008
Revised 30 June 2008
Accepted 1 July 2008
Available online 8 July 2008

Keywords:
HIV-1 integrase inhibitors
Aryl diketoacid
Strand transfer
Dimer
Conformationally constrained linker
Orientation
Substitution effect

ABSTRACT

Aryl diketoacids (ADK) and their bioisosteres are among the most promising HIV-1 integrase (IN) inhibitors. Previously, we designed a series of ADK dimers as a new class of IN inhibitors that were hypothesized to target two divalent metal ions on the active site of IN. Herein we present a further structure–activity relationship (SAR) study with respect to the substituent effect of the ADK and the dimerization with conformationally constrained linkers such as piperazine, 4-amino-piperidine, piperidin-4-ol, and *trans*-cyclohexan-1,4-diamine. The substituents on the phenyl ring as well as the spatial orientation of the two diketo units were observed to play important roles in the IN inhibitory potency. The hydrophobic group was an optimal substitution at the 3-position of the aryl ring. The piperazine and 4-amino-piperidine linkers brought about the most potent analogs among the hydrophobic group or halogen substituted ADK dimers. The docking studies suggested that the bulky hydrophobic substitution at 3-phenyl ring and the linker of 4-amino-piperidine were beneficial for adopting an active conformation to achieve strong interactions with the active site Mg^{2+} and the key residue E152 within the catalytic core domain. This study is a significant extension of our previous report on the dimeric ADK-containing IN inhibitors, providing a new promising template for further lead optimization.

1. Introduction

Human immunodeficiency virus type 1 (HIV-1) encodes three enzymes that are required for viral replication: reverse transcriptase, protease, and integrase (IN). Although drugs targeting reverse transcriptase and protease are in wide use and have shown effectiveness particularly when employed in combination,[1] the search for new anti-HIV-1 agents continues to develop drugs capable of overcoming toxicity and resistance by targeting alternate sites in the viral life cycle.[2] IN has emerged as an attractive target, because it is required for stable infection and has no cellular homologues.[3] The function of IN is to catalyze integration of proviral DNA, resulting from the reverse transcription of viral RNA, into the host genome. This is achieved in a stepwise fashion by endonucleolytic processing of proviral DNA (termed 3′-processing) within a cytoplasmic preintegration complex, followed by translocation of the complex into the nuclear compartment where integration of 3′-processed proviral DNA into host DNA occurs in a 'strand transfer' reaction.

IN is composed of three structural and functional domains, each capable of forming a dimer.[3] The N-terminal domain (residues 1–50) contains the conserved HHCC motif that binds one atom of zinc. This region is involved in protein–protein interaction and contributes to the specific recognition of viral DNA ends. The core or catalytic domain (residues 50–212) contains the highly conserved DDE motif (D64, D116, and E152) present in all retroviral integrases. Mutation of any one of these three acidic residues abolishes IN enzymatic activities and viral replication. The two D64 and D116 residues form a coordination complex with a divalent metal (Mg^{2+} or Mn^{2+}). Because a second metal has been observed in an ASV integrase crystal structure,[4] and because of the two-metal structure for polynucleotide transferases,[5] it has been proposed that a second metal (Mg^{2+} or Mn^{2+}) can be coordinated between D116 and E152 once IN binds its DNA substrate(s).[6,7] It is therefore likely that the metal(s) coordinate(s) IN and the phosphodiester backbone of the DNA substrate(s) during the 3′-processing and strand transfer steps. The C-terminal domain (residues 212–280) is the least conserved IN domain. It is involved in DNA binding and IN oligomerization, which seems necessary for the integration

* Corresponding authors. Tel.: +1 323 442 2341; fax: +1 323 442 1390 (N.N.); tel./fax: +86 21 50806876 (Y.-Q.L.).
E-mail addresses: neamati@usc.edu (N. Neamati), yqlong@mail.shcnc.ac.cn (Y.-Q. Long).

0968-0896/$ - see front matter © 2008 Elsevier Ltd. All rights reserved.
doi:10.1016/j.bmc.2008.07.008

process. These three domains of IN are required for in vitro 3′-end processing and strand transfer.

Among an impressive number of synthetic IN inhibitors reported, aryldiketo (ADK) containing compounds are the most promising that potently block integration in extracellular assays and exhibit good antiviral activity against HIV-infected cells.[8–10] ADK-based inhibitors show selective inhibition of the strand transfer reaction relative to the 3′-processing step and may function by competing with host DNA in binding to the IN proviral DNA complex.[11,12] However, the variation on the aromatic portion was shown to alter the mode of action leading to reduced strand transfer selectivity.[13] Several IN inhibitors containing the aryl diketo motif have been tested in the clinic (Fig. 1).[14] The first FDA-approved IN inhibitor as anti-HIV drug, MK-0518 is also derived from the aryl diketo scaffold.[15]

Based on the X-ray crystal structure of the IN core domain complexed with an ADK-containing inhibitor, 5CITEP,[16] we designed and synthesized a series of novel dimeric diketo containing inhibitors of IN with the notion that such dimeric compounds may simultaneously bind to two divalent metal ions on the active site of IN.[17] The two diketo subunits separated by uniquely designed linkers can potentially chelate two metal ions that are either provided from one IN active site or two active sites juxtaposed together in a higher order tetramer. Indeed, these aryl diketoacid dimers are highly potent against purified IN with varied selectivity for strand transfer, and that some of the analogues exert potent inhibition on the cytopathic effect of HIV-1 in infected CEM cells.[17] The modeling studies revealed that these dimeric diketo containing inhibitors of IN function by targeting two divalent metal ions on the active site of IN. Furthermore, the dimerization linker was observed to modulate the activity of the resulting dimeric aryldiketo containing IN inhibitors by means of securing the distance and orientation of the two separated diketo moieties. Among the linear and cyclic diamino linkers studied, the piperazine appeared to be the best linker for the amide-linked ADK dimers.

Since the ADK dimer represents a new class of IN inhibitors by targeting two divalent metal ions on the active site of IN, and the emergence of viral strains resistant to clinically studied IN inhibitors and the dynamic nature of the HIV-1 genome demand a continued effort toward the discovery of novel inhibitors, we were intrigued to design second generation ADK dimer class of IN inhibitors focused on the orientation of various cyclic linkers. Piperazine, 4-amino-piperidine, piperidin-4-ol, and *trans*-cyclohexan-1,4-diamine were employed as the dimerization linker to explore the geometric requirements for optimal IN inhibitory activity. The substituent effect of the phenyl ring was examined as well, since previous study indicated that the aromatic portion was responsible for the strand transfer selectivity.[13]

In order to better understand the role of different substituents and linker orientation on activity of the ADK dimer, first, positions 2, 3, and 4 of the phenyl moiety in the aryl diketoacid were initially explored to determine optimal substituent. Second, the inhibitory activity of the corresponding β-diketo ester or amide was evaluated in order to establish a coherent SAR among these compounds. Third, various cyclic linkers are investigated to determine the optimal positioning of the two diketo subunits. These structural modifications led to compounds **1**–**13** (**a**,**b**) and **1**,**3**,**4**,**9**–**11** (**c**,**d**,**e**,**f**) (Fig. 2). The present article is focused on the synthesis and SAR analysis of cyclic diamino-linked ADK dimers bearing electron-donating or electron-withdrawing group to address additional elements of structure–inhibitory activity.

2. Synthesis

The monomer was conveniently synthesized by using our previously developed methodology.[18] As shown in Scheme 1, differently substituted acetophenones were oxalylated by dimethyl oxalate in the presence of sodium *tert*-butoxide, affording β-diketo esters **1**–**12a** in high yields. Hydrolysis of the methyl esters by aqueous sodium hydroxide produced β-diketo acids **1**–**12b** with various substituent on the phenyl ring.

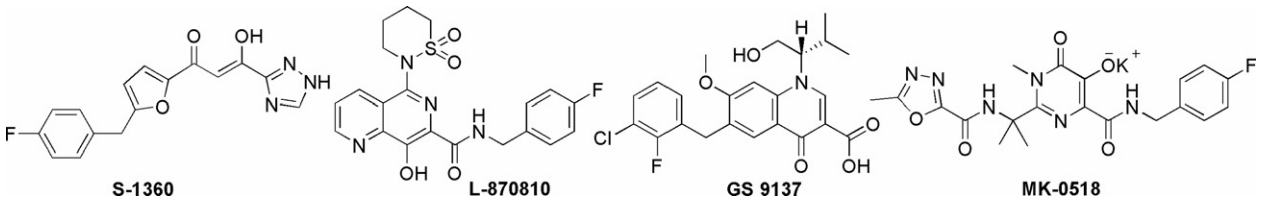

Figure 1. The structures of selected ADK-based clinically studied IN inhibitors.

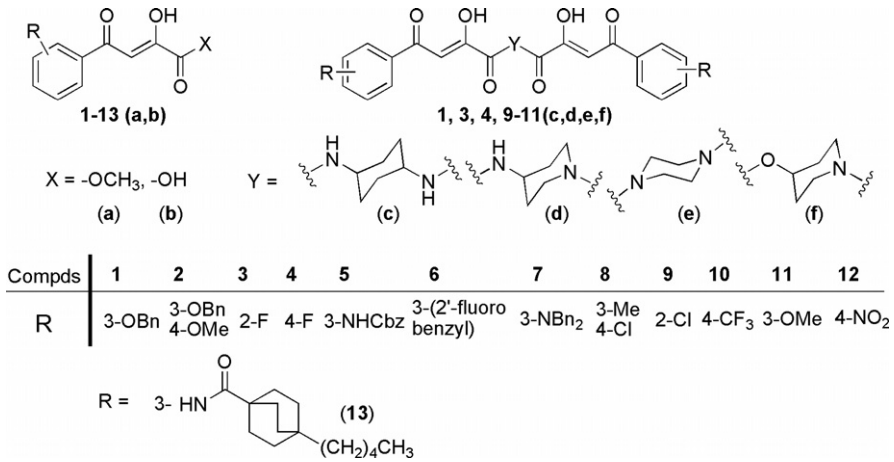

Figure 2. The structures of aryl diketoacid derivatives with variations on the substitution of the aromatic ring, and the linker.

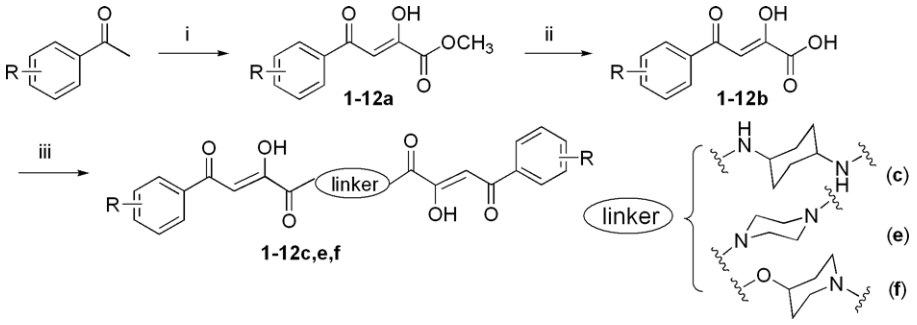

Scheme 1. Reagents and conditions: (i) *t*-BuONa, $(CH_3OOC)_2$, THF, 0 °C–rt; (ii) dioxane, 1 N NaOH, rt; (iii) HOAT, HATU, DIPEA, diamine, DMF or a—$SOCl_2$, CH_2Cl_2, a drop of DMF, 0 °C–rt; b—pyridine, diamine or 4-hydroxyl-piperidine, CH_2Cl_2.

Except for the piperidin-4-amino-linked dimer which required a separate double coupling (Scheme 2), the synthesis of ADK dimers employing cyclohexane-1,4-diamine, piperazine, or piperidin-4-ol as the linker was accomplished by coupling the monomer **1**–**12b** with the cyclic diamine in the presence of HOBt and EDCI or $SOCl_2$ and cat. DMF, affording the corresponding amide-linked dimers **1**–**12c**,**e**,**f** (Scheme 1).

As depicted in Scheme 2, the similar coupling method was applied to the synthesis of piperidin-4-amino-linked dimer **1**–**12d** in a stepwise fashion. Since the linker of 4-amino-piperidine was prepared in an N^1-Boc protected form (compound **14**), the coupling was conducted twice separated by a deprotection reaction.

The linkers of 4-amino-piperidine and 4-hydroxypiperidine were prepared from the common intermediate of *tert*-butyl 4-oxo-piperidine-1-carboxylate **15** via a different reduction approach, as shown in Scheme 3. The N-protection of the commercially available piperidine-4,4-diol hydrochloride with Boc readily yielded the key intermediate **15**, which was converted to *tert*-butyl 4-amino-piperidine-1-carboxylate **14** by palladium-catalyzed hydrogenation in the ammonia saturated methanol, or *tert*-butyl 4-hydroxypiperidine-1-carboxylate by the sodium boron hydride reduction.

It is worth describing separately the synthesis of the aryl diketo acid **13b** bearing a bulky hydrophobic moiety (Scheme 4). The

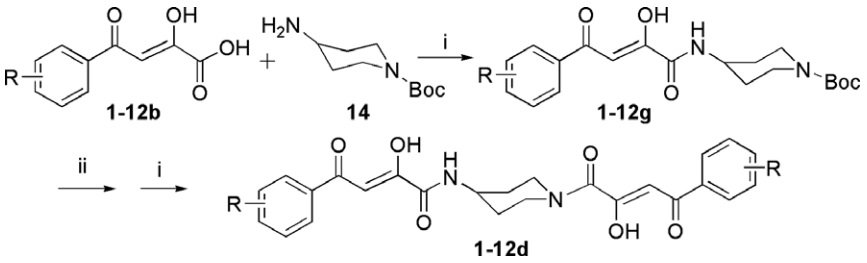

Scheme 2. Reagents and conditions: (i) HOAT, HATU, DIPEA, DMF or a—$SOCl_2$, CH_2Cl_2, a drop of DMF, 0 °C–rt; b—pyridine, alkylamine, CH_2Cl_2, rt; (ii) TFA, CH_2Cl_2, rt.

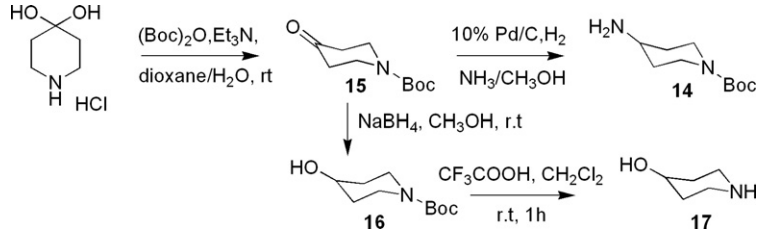

Scheme 3.

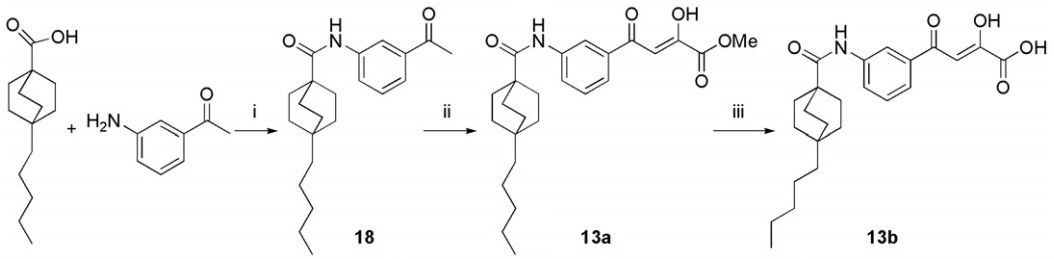

Scheme 4. Reagents and conditions: (i) HBTU, HOBT, DIPEA, CH_2Cl_2, 0 °C–rt; (ii) *t*-BuONa, $(CH_3OOC)_2$, THF–DME, 0 °C–rt; (iii) THF/MeOH, 1 N NaOH, rt.

4-pentylbicyclo[2.2.2]octane-1-carboxylic acid was coupled with 3-amino-acetophenone to give the precursor of *N*-(3-acetylphenyl)-4-pentylbicyclo[2.2.2]octane-1-carboxamide **18**, which underwent the oxalylation and hydrolysis as described previously to afford the desired 2,4-dioxo-4-(3-(4-pentylbicyclo[2.2.2]octane-1-carboxamido)phenyl)butanoic acid **13b**.

3. Results and discussion

3.1. Hydrophobic group of the phenyl substitution is beneficial for the interaction of the ADK compound with the IN enzyme

The substitution of the phenyl portion within the ADK structure was examined first. As shown in Table 1, all aryl diketo containing compounds showed preferential inhibition of strand transfer versus 3′-processing (compounds **1**–**13a**,**b**), and the methyl ester form was significantly less potent than the free acid congener (compounds **1a** vs **1b**, **2a** vs **2b**, **3a** vs **3b**), in which the carboxyl hydroxyl group might be involved in the binding with the host DNA site within IN. This observation is consistent with previous findings.[19,20] Although ADK inhibitors are generally characterized by high strand transfer selectivity, when the phenyl ring was substituted by an additional 2,4-diketobutyric acid group at the 3- or 4-position, the resulting bis-diketo acid analogues displayed enhanced 3′-processing inhibitory potencies, such that selectivity toward strand transfer was remarkably decreased.[20] Literature study has examined the aspects of both the left and right portions of the β-diketopropyl central chain, with focus on the substitution of the whole aromatic moiety with phenyl, indolyl, or quinolyl ring.[20] Our current study is complementary to this report in exploring a wider range of the substituent structure on the phenyl portion in the context of ADK dimers.

In this study, of the 3-, 4-, or 3,4-disubstituted phenyl diketoacids, the best inhibitory activity was exhibited by compounds **1b**, **2b**, and **6a**, which carry a bulky and hydrophobic group at 3-position of the phenyl ring. The 3-benzyloxy substituent on the phenyl moiety displayed highest affinity-enhancing effect (compounds **1b** and **2b**, IC_{50} < 0.4 μM for strand transfer reaction). The 3-(2′-fluorobenzyl) group and 3-benzyloxycarbonylamino group are favored for the strand transfer inhibition for the same reason (IC_{50} = 0.6 and 7 μM for compounds **6a** and **5a**, respectively). Furthermore, the hydrophobic substituent only at 3-position slightly increased the 3′-processing inhibitory potency, resulting in some loss of strand transfer selectivity (IC_{50} = 19 and 26 μM against 3′-processing for compounds **1b** and **6a**, respectively). However, an additional hydrophobic group substituted at 4-position restored the strand transfer selectivity to some extent with retention of the significant strand transfer inhibitory potency (3-benzyloxy-4-methoxy **2b**, IC_{50} = 55 and <0.4 μM for 3′-processing and strand transfer, respectively; 3-methyl-4-chloro **8b**, IC_{50} = 94 and 4.7 μM for 3′-processing and strand transfer, respectively). But introduction of a bulky hydrophobic group such as dibenzylamino at 3-position caused a significant loss of strand transfer inhibitory activity (**7a**, IC_{50} > 100 μM), which might be due to steric hindrance. Probably for a similar reason, the bulky hydrophobic 4-pentylbicyclo[2.2.2]octane-1-carboxamido group (**13b**) substituted at 3-position of the phenyl ring conferred only moderate activity against strand transfer reaction (**13b**, IC_{50} = 14 μM). The following

Table 1
Inhibitory potencies of the aryl diketoacid derivatives against the HIV-1 integrase[a]

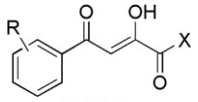

1-13a,b

Compound	R	X	Inhibition of integrase catalytic activities	
			3′-Processing IC_{50} (μM)	Integration IC_{50} (μM)
1a	3-OBn	OCH_3	>100	14
1b		OH	19 ± 5	<0.4
2a	3-OBn, 4-OMe	OCH_3	>100	16
2b		OH	55 ± 6	<0.4
3a	2-F	OCH_3	>100	>100
3b		OH	>100	58 ± 6
4a	4-F	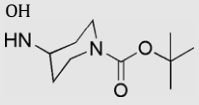	>100	>100
4g			>100	100
5a	3-NHCbz	OCH_3	99	7
6a	3-(2′-Fluorobenzyl)	OCH_3	26 ± 11	0.6
7a	3-NBn_2	OCH_3	>100	>100
8b	3-Me, 4-Cl	OH	94 ± 6	4.7
9b	2-Cl	OH	>100	17 ± 5
10b	4-CF_3	OH	>100	33 ± 12
11b	3-OMe	OH	>100	27 ± 6
12b	4-NO_2	OH	>100	45 ± 4
13b	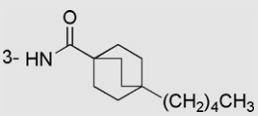	OH	>100	14 ± 1
Reference compound[b]	H	OH	>100	24.2, 25

[a] Values were determined as described in Section 6.
[b] From Ref. 20.

molecular modeling indicated that the crowded substitution on the aryl ring would hamper the interaction of the aromatic portion with the binding cavity.

Accordingly, the electron-withdrawing group or polar group was deleterious to the IN inhibition. The replacement of the benzyloxy group with a trifluoromethyl (**10b**) or a nitro group (**12b**) at 4-position reduced strand transfer potency by approximately 100-folds. The halogen played a different role, among which the fluoro group at 2- (**3a**,**b**) or 4-position (**4a**,**b**) was disfavored, while the chloro group at 2-position gave a slight increase in strand transfer inhibitory activity (**9b**, IC_{50} = 17 μM) compared to the unsubstituted congener (reference compound, IC_{50} = 25 μM).

3.2. The constrained cyclic linker potentiates the IN inhibition of the ADK compounds

In order to investigate the orientation effect of the linker on the ADK inhibition against IN, three cyclic diamines and the 4-hydroxypiperidine were examined as linkers to construct the ADK dimers. As shown in Table 2, the resulting amide-linked constrained ADK dimers are more potent than the corresponding monomers. Of note, the blockade of the carboxy hydroxyl of the ADK dimer by conversion to its amide was accompanied with loss of potency, so the activity comparison was based on the ADK ester monomer instead of the free acid. In this regard, all conformationally constrained amide-linked ADK dimers gained an enhancement of the IN inhibitory activity, but the potentiating effect on the 3′-processing inhibitory potency is not as significant as the bis-diketo acid analogues which bear two free carboxyate groups.[13,19] They may function via a different mechanism.[13,17]

For the most active ADK compound in this series, that is, (*Z*)-4-(3-(benzyloxy)phenyl)-2-hydroxy-4-oxobut-2-enoic acid (**1b**), the 4-amino-piperidine (**1d**) displayed the best potency among the four cyclic linkers (**1c**–**f**). Compared to the (*Z*)-methyl 4-(3-(benzyloxy)phenyl)-2-hydroxy-4-oxobut-2-enoate (**1a**, IC_{50} = 14 and >100 μM for strand transfer and 3′-processing, respectively), the 4-amino-piperidine linker achieved more than 35-fold enhancement in the strand transfer inhibitory potency and meanwhile renders the 3′-processing inhibition effective (**1d**, IC_{50} = <0.4 and 23 μM for strand transfer and 3′-processing, respectively). The second best linker was piperazine (**1d**), which conferred potent strand transfer inhibition (IC_{50} = 1.8 μM) while maintaining the 3′-processing inhibitory activity at moderate level (IC_{50} = 56 μM). The 4-hydroxypiperidine and cyclohexane-1,4-diamine with IC_{50} values of 3 and 7 μM for strand transfer, respectively, displayed similar potency.

Examining the other conformationally restricted dimers (**3**,**4**,**9**,**10**,**11c**–**e**), the order of the cyclic linker with respect to the potentiating effect varied for variously substituted ADK. However, the piperazine behaved as the best cyclic linker in most cases except for 2-chloro substituted phenyl diketoacid analog. Since the conformationally constrained linker positioned the two ADK units into close proximity, the substituent on the phenyl ring might bring about the repulsion with another functionality, which might distort the orientation of the ADK unit. So the final spatial arrangement of the two ADK moieties was decided by both the cyclic linker and the phenyl substitution. In the case of electron-donating group or halogen substituted phenyl diketo acids, 4-amino-piperidine and piperazine can achieve an optimal orientation for the two ADK subunits into the IN binding cavity. These observations were rationalized by docking studies as described below.

4. Docking studies

The above observations can be reasonably rationalized by molecular modeling. To predict the binding conformation of ADK analogues, all newly synthesized analogues were docked into the active site of IN using GOLD program (CCDC, Cambridge, UK).[21] Interestingly, ADK monomers with a free carboxylate group adopted a similar binding conformation. Herein taken **2b**, one of the most potent ADK analogues, as an example. As shown in Figure 3B, the diketoacid group of compound **2b** is interacting with the active site Mg^{2+}. The β-keto ($C{=}O\cdots Mg^{2+}$ 2.15 Å) and enol ($C{-}OH\cdots Mg^{2+}$ 1.85 Å) oxygens formed strong coordinate bonds with the active site Mg^{2+}. The hydrophobic benzyloxy substituent on 3-position of the aryl ring occupies a cavity surrounded by E152, N155, K156, and K159.

For the cyclic diamine-linked dimers, the 4-amino-piperidine linker containing compound **1d** adopted an interesting binding mode inside the active site of IN. One of the aryl β-keto units of the dimeric ADK **1d** established strong interactions with the active site Mg^{2+} (Fig. 3C). Similar to compound **2b**, the hydrophobic benzyloxy substituent on 3-position of the aryl ring of compound **1d** occupies a cavity surrounded by E152, N155, K156, and K159. Additionally, the 4-amino-piperidine linker and the second aryl β-keto unit of dimeric ADK occupies an area surrounded by amino acid residues E92, T93, N117, S119, and T122. Interestingly, inactive compound **9e** adopted a very different bound conformation inside the active site of IN. Due to the absence of bulky hydrophobic substituent at 3-position of the phenyl ring, the compound occupied a large cavity inside the active site near the Mg^{2+}. Consequently, contrary to active compounds **2b** and **1d**, compound **9e** did not make an interaction with active site Mg^{2+}.

The predicted binding modes of the active and inactive monomeric and dimeric ADK analogues demonstrate that the β-diketo-acid part interacts with the active site Mg^{2+}, while the inactive dimer lacks such interactions. The well tolerated and potency-enhancing hydrophobic substituent on the 3-position of the aryl ring occupies a cavity close to one of the catalytically important residues E152. The bound conformation of compound **9e** indicates the importance of a bulky substitution on 3-position of the aryl ring. The predicted binding modes also reveal that further bulky substitutions on the aryl ring other than 3-position could hamper potency of the compounds.

5. Conclusions

In this study, we investigated the substitution and orientation effects of amide-linked ADK dimers as a novel class of IN inhibitors. The hydrophobic group at 3-position of phenyl ring was important for IN inhibition. The 4-amino-piperidine and piperazine behaved as the best cyclic linkers for the amide-linked ADK dimers to achieve potent inhibitory activity against 3′-processing reaction. Docking studies revealed that the conformationally constrained linker of 4-amino-piperidine positioned the two ADK subunits properly inside the binding pocket of IN to establish interactions with the active site Mg^{2+} and the key residue E152 within the catalytic core domain. This study is a significant extension of our previous report on the dimeric ADK-containing IN inhibitor, providing promising new templates for further development of potent inhibitors directed toward different sites.

6. Experimental

6.1. General synthetic methods

Unless otherwise stated, the ^1H NMR spectra were recorded on a Varian 300-MHz or 400-MHz spectrometer. The data are reported in parts per million relative to TMS and referenced to the solvent. Elemental analyses were obtained using a Vario EL spectrometer. Melting points (uncorrected) were determined on a Buchi-510

Table 2
Inhibitory potencies of the aryl diketoacid dimers against the HIV-1 integrase catalytic activity

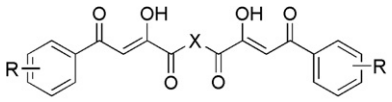

1-12c, d, e, f

Compound	R	X	Inhibition of integrase catalytic activities	
			3′-Processing IC_{50} (μM)	Strand transfer IC_{50} (μM)
1c	3-OBn	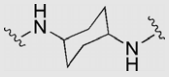	>100	7
1d		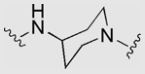	23 ± 6	<0.4
1e		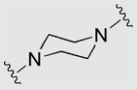	56 ± 25	1.8
1f		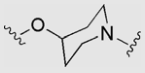	91 ± 40	3 ± 1
3c	2-F	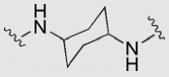	>100	55 ± 15
4c	4-F	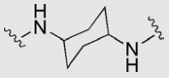	>100	35.5 ± 0.5
4d		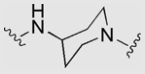	>100	88 ± 12
4e		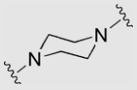	>100	29 ± 8
9c	2-Cl	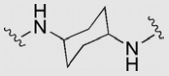	92 ± 9	30 ± 10
9d		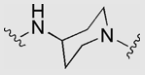	99 ± 2	31 ± 12
9e		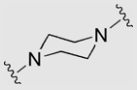	>100	>100
10c	4-CF_3	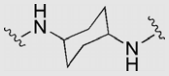	>100	41 ± 16
10e		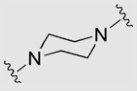	>100	25 ± 14
11c	3-OMe	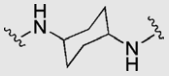	>100	26 ± 7
11d		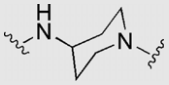	>100	53 ± 15
11e		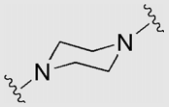	>100	26 ± 8

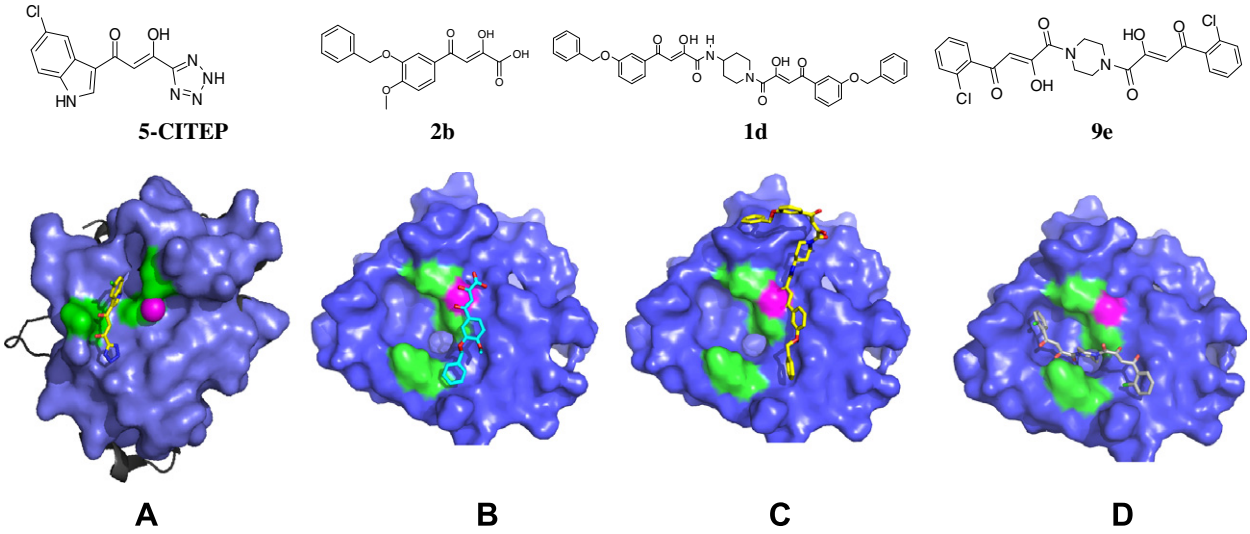

Figure 3. (A) The diketoacid bioisostere 5-CITEP bound to the core domain of HIV-1 integrase (1QS4·PDB). (B) The predicted bound conformation of one of the highly active aryl diketoacids (**2b**) inside the active site of HIV-1 integrase (1BIS·PDB). (C) The predicted bound conformation of highly active dimeric aryl diketo analogue (**1d**) inside the active site of HIV-1 integrase. (D) The predicted bound conformation of one of the inactive compounds (**9e**) inside the active site of HIV-1 integrase. The blue surface shows the active site region of the HIV-1 integrase. Green surface represents catalytic triad DDE. The magenta surface represents active site Mg^{2+}.

capillary apparatus. IR spectra were recorded on Bio-Rad FTS-185 spectrometers. The MS and HRMS (ESI) spectra were obtained on an APEXIII 7.0 T FTMS mass spectrometer. Degree of rotation was measured by P-1030 (A012360639) automatic polarimeter. The flash column chromatography was performed on silica gel H (10–40 μm). Anhydrous solvents were obtained by standard procedure.

Analytical HPLC for selected compounds were performed on two systems, using Vydac C18 column (10 × 250 mm). UV detector, 254 nm. System A: Solvent system used was 0.05% TFA in methanol and 0.05% TFA in water, gradient 30–90% over 20 min @ 2 mL/min. System B: Solvent system used was 0.05% TFA in 95% acetonitrile and 0.05% TFA in water, gradient 30–90% over 20 min @ 2 mL/min.

6.2. Materials, chemicals, and enzymes

All compounds were dissolved in DMSO and the stock solutions were stored at −20 °C. The γ[^{32}P]ATP was purchased from either Amersham Biosciences or ICN. The expression systems for the wild-type IN and soluble mutant IN^{F185KC280S} were generous gifts of Dr. Robert Craigie, Laboratory of Molecular Biology, NIDDK, NIH, Bethesda, MD.

6.3. Preparation of oligonucleotide substrates

The oligonucleotides 21top, 5′-GTGTGGAAAATCTCTAGCAGT-3′ and 21bot, 5′-ACTGCTAGAGATTTTCCACAC-3′ were purchased from Norris Cancer Center Core Facility (University of Southern California) and purified by UV shadowing on polyacrylamide gel. To analyze the extent of 3′-processing and strand transfer using 5′-end labeled substrates, 21top was 5′-end labeled using T_4 polynucleotide kinase (Epicentre, Madison, WI) and γ[^{32}P]ATP (Amersham Biosciences or ICN). The kinase was heat-inactivated and 21bot was added in 1.5-molar excess. The mixture was heated at 95 °C, allowed to cool slowly to room temperature, and run through a spin 25 mini-column (USA Scientific) to separate annealed double-stranded oligonucleotide from unincorporated material.

6.4. Integrase assays

To determine the extent of 3′-processing and strand transfer, wild-type IN was preincubated at a final concentration of 200 nM with the inhibitor in reaction buffer (50 mM NaCl, 1 mM HEPES, pH 7.5, 50 μM EDTA, 50 μM dithiothreitol, 10% glycerol (w/v), 7.5 mM $MnCl_2$, 0.1 mg/mL bovine serum albumin, 10 mM 2-mercaptoethanol, 10% dimethyl sulfoxide, and 25 mM MOPS, pH 7.2) at 30 °C for 30 min. Then, 20 nM of the 5′-end ^{32}P-labeled linear oligonucleotide substrate was added, and incubation was continued for an additional 1 h. Reactions were quenched by the addition of an equal volume (16 μL) of loading dye (98% deionized formamide, 10 mM EDTA, 0.025% xylene cyanol and 0.025% bromophenol blue). An aliquot (5 μL) was electrophoresed on a denaturing 20% polyacrylamide gel (0.09 M tris–borate, pH 8.3, 2 mM EDTA, 20% acrylamide, 8 M urea).

Gels were dried, exposed in a PhosphorImager cassette, and analyzed using a Typhoon 8610 Variable Mode Imager (Amersham Biosciences) and quantitated using ImageQuant 5.2. Percent inhibition (%I) was calculated using the following equation:

$$\%I = 100 \times [1 - (D - C)/(N - C)]$$

where C, N, and D are the fractions of 21-mer substrate converted to 19-mer (3′-processing product) or strand transfer products for DNA alone, DNA plus IN, and IN plus drug, respectively. The IC_{50} values were determined by plotting the logarithm of drug concentration versus percent inhibition to obtain concentration that produced 50% inhibition.

6.5. Docking studies

The structures of all the compounds (Tables 1 and 2) were built and minimized using Catalyst (Accelrys, Inc.).[22] All compounds were modeled in their enol tautomeric form as this form is considered biologically relevant. Compounds with a free acid group were modeled as carboxylates. The poling algorithm implemented within Catalyst was used to generate conformations for all the compounds.[23] For each compound all feasible unique conformations were generated over a 20 kcal/mol range of energies using the best flexible conformation generation method in Catalyst.[24,25] The subunit B of the core domain X-ray structure of IN (PDB 1BIS) in which all the active site amino acid residues were resolved was chosen for docking purpose.[26] A Mg^{2+} ion was placed in the active site between carboxylate oxygen atoms of amino acid residues D64 and D116 considering the geometry of the Mg^{2+} ion that was present

in the subunit A of the IN in PDB 1BIS and subunit A in IN–5CITEP complex X-ray structure (PDB 1QS4).[16] All the water molecules present in protein were removed, and hydrogen atoms were added to the protein considering appropriate ionization states for both the acidic and basic amino acid residues. Docking was performed using version 3.2 of the GOLD: Genetic Optimization for Ligand Docking (Cambridge Crystallographic Data Centre) software package.[21,27,28] A 20 Å radius active site was defined considering the carboxylate oxygen atom (OD1) of amino acid residue D64 as the center of the active site. All the compounds were docked into the active site of the IN. On the basis of the GOLD fitness score, for each molecule, a bound conformation with high fitness score was considered as the best bound conformation. All docking runs were carried out using standard default settings with a population size of 100, a maximum number of 100,000 operations, and a mutation and crossover rate of 95. The fitness function that was implemented in GOLD consisted basically of H-bonding, complex energy, and ligand internal energy terms.

6.6. General procedure for the synthesis of monomeric aryl diketo acids

To a stirred mixture of *t*-BuONa (2.5 equiv) and dimethyl oxalate (2.0 equiv) in anhydrous THF at 0 °C was added dropwise aryl methyl ketone (1.0 equiv) in DME. The resulting orange-yellow mixture was stirred at room temperature for 1.5 h at most. The reaction mixture was quenched with 1.0 mol/L aqueous HCl and extracted with CH_2Cl_2. The combined organic layers were washed with saturated aqueous $NaHCO_3$ and brine, respectively, dried over Na_2SO_4 and concentrated under vacuum. Purification by silica gel flash chromatography provided the desired 4-(substituted phenyl)-4-oxo-2-hydroxy-2-butenoic acid methyl esters **1**–**13a**.[18] The subsequent hydrolysis of the resulting aryl diketoacid methyl ester readily furnished the corresponding aryl diketoacids **1**–**13b** by 1 N NaOH in MeOH/THF (1:1) at room temperature.

6.6.1. (*Z*)-4-(3-(Benzyloxy)phenyl)-2-hydroxy-4-oxobut-2-enoic acid (1b)

Pale yellow solid, yield 73.0%. ^{1}H NMR (400 MHz, $CDCl_3$): δ 7.61–7.59 (m, 2H); 7.47–7.35 (m, 6H); 7.25–7.23 (m, 1H); 7.15 (s, 1H); 5.14 (s, 2H). EI-MS (*m*/*z*, %): 298 (M^+, 3.0); 91 (100.0). Anal. Calcd for $C_{17}H_{14}O_5$: C 68.45, H 4.73. Found: C 68.52, H 4.38.

6.6.2. (*Z*)-4-(3-(Benzyloxy)-4-methoxyphenyl)-2-hydroxy-4-oxobut-2-enoic acid (2b)

Pale yellow solid, yield 84%. ^{1}H NMR (400 MHz, $CDCl_3$ + CD_3OD): δ 7.79–7.76 (m, 2H); 7.64–7.52 (m, 5H); 7.15 (d, 1H, *J* = 8.8 Hz); 7.01 (s, 1H); 5.44 (s, 2H); 4.16 (s, 3H). EI-MS (*m*/*z*, %): 328 (M^+, 8.0); 91 (100.0). HR-EIMS calcd for $C_{18}H_{16}O_6$: 328.0947, found: 498.0950. Calcd for $C_{18}H_{16}O_6$: C 65.85, H 4.91. Found: C 65.85, H 4.84.

6.6.3. (*Z*)-4-(2-Fluorophenyl)-2-hydroxy-4-oxobut-2-enoic acid (3b)

Pale yellow solid, yield 86%. ^{1}H NMR (400 MHz, $CDCl_3$): δ 8.00–7.95 (m, 1H); 7.61–7.55 (m, 1H); 7.32–7.27 (m, 1H); 7.21–7.18 (m, 2H). EI-MS (*m*/*z*, %): 210 (M^+, 4.0); 165 (100.0); 123 (64.0). Anal. Calcd for $C_{10}H_7FO_4$: C 57.15, H 3.36. Found: C 57.21, H 3.36.

6.6.4. (*Z*)-4-(4-Fluorophenyl)-2-hydroxy-4-oxobut-2-enoic acid (4b)

Pale solid, yield 88%. ^{1}H NMR (300 MHz, $CDCl_3$): δ 8.04 (m, 2H); 7.21 (m, 2H); 7.13 (s, 1H). EI-MS (*m*/*z*, %): 210 (M^+, 4.0); 165 (100.0); 123 (56.0). HR-EIMS calcd for $C_{10}H_7FO_4$: 210.0328, found: 210.0324. Analytical HPLC t_R = 22.79 min, purity 99.3% (solvent system A); t_R = 15.433 min, purity 95.4% (solvent system B).

6.6.5. (*Z*)-*tert*-Butyl 4-(4-(4-fluorophenyl)-2-hydroxy-4-oxobut-2-enamido)piperidine-1-carboxylate (4g)

Prepared by the same procedure as the preparation of **11g**, pale yellow solid, yield 96%. ^{1}H NMR (400 MHz, $CDCl_3$): δ 7.95 (d, 1H, *J* = 7.8 Hz); 7.50 (m, 1H); 7.40 (m, 1H); 7.18 (s, 1H); 7.14–7.12 (m, 1H); 7.09 (s, 1H); 4.09–3.96 (m, 3H); 2.91 (m, 2H); 1.98–1.94 (m, 2H); 1.46 (s, 9H); 1.49–1.39 (m, 2H). EI-MS (*m*/*z*, %): 392 (M^+, 10.0). Analytical HPLC t_R = 25.51 min, purity 100% (solvent system A); t_R = 23.19 min, purity 99.9% (solvent system B).

6.6.6. (*Z*)-4-(4-Chloro-3-methylphenyl)-2-hydroxy-4-oxobut-2-enoic acid (8b)

White solid, yield 86.0%. ^{1}H NMR (400 MHz, $CDCl_3$ + CD_3OD): δ 7.89–7.79 (m, 1H); 7.70–7.67 (m, 1H); 7.40–7.28 (m, 1H); 7.10 (s, 1H); 2.38 (s, 3H). EI-MS (*m*/*z*, %): 242 (M^+, 4.0); 240 (M^+, 12.0); 197 (32.0); 195 (96.0); 155 (13.0); 153 (39.0); 69 (100.0). HR-EIMS calcd for $C_{11}H_9ClO_4$: 240.0189, found: 240.0185. Anal. Calcd for $C_{11}H_9ClO_4$: C 54.90, H 3.77. Found: C 55.18, H 4.30.

6.6.7. (*Z*)-4-(2-Chlorophenyl)-2-hydroxy-4-oxobut-2-enoic acid (9b)

White solid, yield 85%. ^{1}H NMR (400 MHz, $CDCl_3$): δ 7.70–7.68 (m, 1H); 7.51–7.46 (m, 2H); 7.42–7.38 (m, 1H); 7.11 (s, 1H). EI-MS (*m*/*z*, %): 228 (M^++2, 4.0); 226 (M^+, 4.0); 191 (38.0); 183 (32.0); 181 (100.0); 141 (14.0); 139 (42.0). Anal. Calcd for $C_{10}H_7ClO_4$: C 53.00, H 3.11. Found: C 53.21, H 3.08.

6.6.8. (*Z*)-2-Hydroxy-4-oxo-4-(4-(trifluoromethyl)phenyl) but-2-enoic acid (10b)

White needle solid, yield 87.0%. ^{1}H NMR (400 MHz, $CDCl_3$): δ 8.11 (d, 2H, *J* = 8.0 Hz); 7.82 (d, 2H, *J* = 8.0 Hz); 7.20 (s, 1H). EI-MS (*m*/*z*, %): 260 (M^+, 3.0); 241 (4.0); 215 (100.0); 173 (45.0); 145 (37.0). HR-EIMS calcd for $C_{11}H_7F_3O_4$: 260.0296, found: 260.0301. Anal. Calcd for $C_{11}H_7$ $F_3O_4 \cdot 0.2CH_2Cl_2 \cdot 0.8CH_3OH$: C 47.60, H 3.53. Found: C 47.33, H 3.34.

6.6.9. (*Z*)-2-Hydroxy-4-(3-methoxyphenyl)-4-oxobut-2-enoic acid (11b)

Pale yellow solid, yield (66.6%). ^{1}H NMR (300 MHz, $CDCl_3$): 7.59 (d, 1H, *J* = 8.0 Hz); 7.51 (s, 1H); 7.43 (d, 2H, *J* = 8.0 Hz); 7.18 (m, 1H); 7.15 (s, 1H); 3.89 (s, 3H). EI-MS (*m*/*z*): 222 (M^+); Anal. Calcd for $C_{11}H_{10}O_5$: C 59.46, H 4.54. Found: C 59.06, H 4.32.

6.6.10. (*Z*)-2-Hydroxy-4-(4-nitrophenyl)-4-oxobut-2-enoic acid (12b)

Yellow solid, yield 75.0%. ^{1}H NMR (400 MHz, $CDCl_3$ + CD_3OD): δ 8.31 (d, 2H, *J* = 8.8 Hz); 8.12 (d, 2H, *J* = 8.8 Hz); 7.08 (s, 1H). EI-MS (*m*/*z*, %): 237 (M^+, 3.0); 192 (100.0); 150 (34.0). Anal. Calcd for $C_{10}H_7NO_6 \cdot 0.6H_2O \cdot 0.4CH_3OH$: C 47.90, H 3.79, N 5.37. Found: C 47.97, H 3.60, N 4.90.

6.6.11. *N*-(*tert*-Butyloxycarbonyl)-4-piperidinol (16)

A stirred solution of the 4-oxo-piperidine-1-carboxylic acid *tert*-butyl ester **15** (0.398 g, 2 mmol) in MeOH (15 mL) was cooled to 0 °C under nitrogen and then treated portionwise with sodium borohydride (0.4 g, 10 mmol) over 0.5 h. The resulting solution was stirred at room temperature for 5 h and then diluted with H_2O (20 mL). The resulting mixture was partitioned between ethyl acetate (50 mL) and washed with brine (50 mL), and then the organic phase was dried over Na_2SO_4, filtered. After removal of the solvent, the residue was purified by column chromatography (petroleum/EtOAc = 3:1) to provide 0.378 g of **16** as white solid in yield of 93.8%. ^{1}H NMR (400 Hz, $CDCl_3$): δ 4.67 (s, 1H); 3.57–3.67 (m, 3H); 2.94 (s, 2H); 1.63–1.69 (m, 2H); 1.40 (s, 9H); 1.18–1.35 (m, 2H).

6.6.12. 1,4-Hydroxypiperidine (17)

At 0 °C, trifluoroacetic acid (1 mL) was added dropwise to the solution of **16** (0.360 g,1.8 mmol) in dry CH_2Cl_2 (3 mL), and then the solution was stirred at room temperature for 1 h, the reaction was monitored by TLC. After removal of the solvent, the residue was treated with 2 N NaOH aq solution, extracted with CH_2Cl_2 (3× 30 mL), washed with saturated brine (20 mL), then the resulting organic phase was dried over anhydrous Na_2SO_4, concentrated to an oil residue **17** (0.175 g), which was used directly for the next step.

6.6.13. *N*-(3-Acetylphenyl)-4-pentylbicyclo[2.2.2]octane-1-carboxamide (18)

HBTU (0.759 g, 2.0 mmol), HOBT (0.270 g, 2.0 mmol), 3-aminoacetophenone (0.135 g, 1.0 mmol) and 4-pentylbicyclo[2.2.2]octane-1-1 carboxylic acid (0.336 g, 1.5 mmol) were dissolved in CH_2Cl_2 (10 mL) at 0 °C and stirred for 10 min, then DIPEA (0.873 mL, 5.0 mmol) was added to the mixture. The reaction mixture was stirred at 0 °C for 2 h, warmed to room temperature and stirred overnight. The reaction mixture was concentrated in vacuo, and the residue was purified by chromatography using PE/EtOAc (5:1) as eluent to give compound **18** as white solid (0.183 g, 36%). ^{1}H NMR (400 MHz, $CDCl_3$): δ 8.03 (t, 1H, J = 1.8 Hz); 7.87 (ddd, 1H, J = 1.0, 2.2, 8.1 Hz); 7.67 (ddd, 1H, J = 1.0, 1.7, 7.7 Hz); 7.40 (t, 1H, J = 7.9 Hz); 2.59 (s, 3H); 1.87–1.83 (m, 6H); 1.47–1.44 (m, 6H); 1.33–1.08 (m, 8H); 0.88 (t, 3H, J = 7.1 Hz).

6.6.14. Methyl2,4-dioxo-4-(3-(4-pentylbicyclo[2.2.2]octane-1-carboxamido)phenyl)butanoate (13a)

Compound **13a** was prepared according to the general method, white solid (0.147 g, 79%). ^{1}H NMR (400 MHz, $CDCl_3$): δ 15.20 (br, 1H); 8.03 (m, 1H); 7.93 (m, 1H); 7.71 (m, 1H); 7.44 (t, 1H, J = 1.8 Hz); 7.37 (s, 1H); 7.06 (s, 1H); 3.94 (s, 3H); 1.88–1.84 (m, 6H); 1.49–1.42 (m, 6H); 1.33–1.01 (m, 8H); 0.88 (t, 3H, J = 7.0 Hz). EI-MS (m/z, %): 427 (M^+, 18.0); 368 (10.0); 341 (8.0); 179 (100).

6.6.15. 2,4-Dioxo-4-(3-(4-pentylbicyclo[2.2.2]octane-1-carboxamido)phenyl)butanoic acid (13b)

Compound **13b** was prepared as white solid (0.077 g, yield 79.0%) according to the general method. ^{1}H NMR (400 MHz, $CDCl_3$): δ 8.14 (s, 1H); 7.83 (d, 1H, J = 7.8 Hz); 7.73 (d, 1H, J = 7.8 Hz); 7.46 (m, 2H); 7.15 (s, 1H); 1.89–1.85 (m, 6H); 1.49–1.45 (m, 6H); 1.31–1.13 (m, 8H); 0.88 (t, 3H, J = 7.1 Hz). EI-MS (m/z, %): 413 (M^+); 341 (36.0); 179 (100.0). Anal. Calcd for $C_{24}H_{31}NO_5$: C 69.71, H 7.56, N 3.39. Found: C 68.01, H 5.21, N 4.02.

6.6.16. 1,1′-(Cyclohexane-1,4-diaminyl)bis(4-(3-(benzyloxy)-phenyl)butane-1,2,4-trione) (1c)

A solution of compound **1b** (0.15 g, 0.5 mmol), EDCI (0.101 g, 0.525 mmol), and HOBt (0.071 g, 0.525 mmol) in dry DMF (1.5 mL) was stirred at 0 °C for 15 min. To this solution was added cyclohexane-1,4-diamine (0.026 g, 0.23 mmol) in dry DMF. The reaction mixture was stirred for 2.5 h at room temperature and then poured into ice-water and extracted with dichloromethane. The combined organic layers were washed with water and brine and dried over Na_2SO_4. The concentration provided the residue which was purified by chromatography using CH_2Cl_2/CH_3OH (60:1) as eluent to give compound **1c** as white solid in 68% yield. ^{1}H NMR (400 MHz, $CDCl_3$): δ 15.6 (br, 2H); 7.61 (m, 4H); 7.45–7.35 (m, 12H); 7.21–7.19 (m, 4H); 7.07 (d, 2H, J = 8.4 Hz); 5.13 (s, 4H); 3.88 (s, 2H); 2.13 (m, 4H); 1.45 (m, 4H). EI-MS (m/z): 674 (M^+). Analytical HPLC t_R = 38.40 min, purity 100% (solvent system A); t_R = 33.25 min, purity 98.9% (solvent system B).

6.6.17. *tert*-Butyl 4-(4-(3-methoxyphenyl)-2-hydroxy-4-oxobut-2-enamido)piperidine-1-carboxylate (11g)

HATU (183 mg, 0.48 mmol), HOAT (66 mg, 0.48 mmol), *N*-Boc-4-amino-piperidine (80 mg, 0.40 mmol) and 4-(3-methoxyphenyl)-2,4-dioxo-butyric acid (94 mg, 0.42 mmol) were dissolved in 4.0 mL THF at 0 °C and stirred for 10 min, then DIPEA (0.084 mL, 0.48 mmol) was added to the mixture. The reaction mixture was stirred at 0 °C for 2 h, then warm to room temperature and stirred overnight. The reaction mixture was concentrated in vacuo, and the residue was purified by chromatography using $CHCl_3/CH_3OH$ (40:1) as eluent to give the product **11g** as pale yellow solid (152 mg, 94.0%). ^{1}H NMR (400 MHz, $CDCl_3$): δ 7.59 (d, 1H, J = 7.8 Hz); 7.50 (m, 1H); 7.40 (m, 1H); 7.18 (s, 1H); 7.14–7.12 (m, 1H); 7.09 (s, 1H); 4.09–3.96 (m, 3H); 3.87 (s, 3H); 2.91 (m, 2H); 1.98–1.94 (m, 2H); 1.46 (s, 9H); 1.49–1.39 (m, 2H). EI-MS (m/z, %): 404 (M^+, 9.0); 348 (2.0); 304 (2.0); 177 (42.0); 82 (100.0). HR-EIMS calcd for $C_{21}H_{28}N_2O_6$: 404.1958, found: 404.1947.

6.6.18. 4-(3-Methoxyphenyl)-*N*-{1-[4-(3-methoxyphenyl)-2,4-dioxo-butyryl]-piperidin-4-yl}-2,4-dioxo-butyramide (11d)

To the solution of compound **11g** (0.1 g, 0.247 mmol) in methylene chloride (4.0 mL) was added trifluoroacetic acid (2.0 mL). The mixture was stirred at room temperature for 2 h. After the removal of the solvent and trifluoroacetic acid under reduced pressure, 2 N NaOH was added and extractive work up with EtOAc. The organic layer was washed with saturated $NaHCO_3$, brine and dried over Na_2SO_4 and the solvent was removed under vacuum to give a solid. The solid above, HATU (113 mg, 0.297 mmol), HOAT (41 mg, 0.297 mmol), **11b** (75 mg, 0.247 mmol) and 4-(3-methoxyphenyl)-2,4-dioxo-butyric acid (58 mg, 0.26 mmol) were dissolved in 2.5 mL THF at 0 °C and stirred for 10 min, then DIPEA (0.053 mL, 0.297 mmol) was added to the mixture. The reaction mixture was stirred at 0 °C for 2 h, then warm to room temperature and stirred overnight. The reaction mixture was concentrated in vacuo, and the residue was purified by chromatography using $CHCl_3/CH_3OH$ (40:1) as eluent to give the product **11d** as glassy solid (70 mg, yield 56.0%). ^{1}H NMR (300 MHz, $CDCl_3$): δ 7.57–7.54 (m, 1H), 7.47 (m, 2H), 7.44–7.36 (m, 3H), 7.24–7.22 (m, 1H), 7.16 (s, 1H) 7.09 (dt, J = 1.8, 15.9, 2H), 6.53 (s, 1H), 4.53 (m, 1H), 4.08 (m, 2H), 3.83 (s, 3H), 3.80 (s, 3H), 3.25 (t, J = 11.7, 1H), 2.94 (t, J = 11.7, 1H), 2.07–2.02 (m, 2H), 1.63–1.55 (m, 2H), 1.25–1.21 (m, 1H). ESI-MS m/z: 508.2 $(M)^+$. Anal. ($C_{27}H_{28}O_6N_2$): C 63.77, H 5.55, N 5.51. Found: C 63.53, H 5.70, N 5.51.

6.6.19. 4-(3-Benzyloxy-phenyl)-*N*-{1-[4-(3-benzyloxy-phenyl)-2,4-dioxo-butyryl]-piperidin-4-yl}-2,4-dioxo-butyramide (1d)

Compound **1d** was prepared in a similar fashion as described for **11d**, yields 65.0%, yellow glassy solid. ^{1}H NMR (400 MHz, $CDCl_3$): δ 7.61–7.59 (m, 2H); 7.54–7.50 (m, 2H); 7.47–7.33 (m, 12H); 7.22–7.16 (m, 4H); 5.12 (s, 4H); 4.57–4.54 (m, 1H); 4.16–4.09 (m, 2H); 3.27 (m, 1H); 2.98–2.83 (m, 1H); 2.08 (m, 2H); 1.60 (m, 2H). EI-MS (m/z, %): 435 (2.0); 226 (16.0); 91 (100.0); 58 (90.0). Analytical HPLC t_R = 25.68 min, purity 96.9% (solvent system A), t_R = 24.49 min, purity 100% (solvent system B).

6.6.20. 4-(3-Benzyloxy-phenyl)-1-{4-[4-(3-benzyloxy-phenyl)-2,4-dioxo-butyryl]-piperazin-1-yl}-butane-1,2,4-trione (1e)

Compound **1e** was prepared in a similar fashion as described for **1c**, as red solid (85–90%). ^{1}H NMR (300 MHz, $CDCl_3$): δ 7.55–7.34 (m, 16H), 7.20–7.16 (m, 2H), 6.63 (s, 2H), 5.12 (s, 4H), 3.78 (s, 8H). ESI-MS m/z: 646.2 $(M)^+$. Anal. ($C_{38}H_{34}O_8N_2$): C 70.58, H 5.30, N 4.33. Found: C 70.42, H 5.10, N 4.18.

6.6.21. 4-(3-Benzyloxy-phenyl)-2,4-dioxo-butyric acid 1-[4-(3-benzyloxy-phenyl)-2,4-dioxo-butyryl]-piperidin-4-yl ester (1f)

To a solution of 4-(3-(benzyloxy)phenyl)-2,4-dioxobutanoic acid (**1b**) (0.297 g, 1.0 mol) in 5 mL dry CH_2Cl_2 were added 0.15 mL $SOCl_2$ and 1 drop of DMF at room temperature for 1.5 h. Then the excess $SOCl_2$ was removed under reduced pressure at 20–30 °C. The residue was dissolved in 5 mL dry CH_2Cl_2 and then was added to a solution of 1,4-hydroxypiperidine (**17**) (0.045 g, 0.45 mol) and 0.2 mL pyridine at 0 °C for 0.5 h. After being stirred at 20–25 °C for 3 h, the reaction mixture was diluted with 20 mL CH_2Cl_2 and then partitioned between dichloromethane (20 mL) and brine (20 mL). The organic layer was separated and dried over Na_2SO_4, filtered and concentrated under reduced pressure to afford **1f** (0.227 g, 68.7%) as yellow solid. Chromatography (silica gel, elution with CH_2Cl_2/CH_3OH = 30:1) provided a light yellow foam solid, ^{1}H NMR (400 Hz, $CDCl_3$): δ 7.42–7.27 (m, 14H); 7.01–7.22 (m, 4H); 5.03 (s, 4H); 3.88 (m, 1H); 3.49 (m,2H); 2.94–3.09 (m, 4H); 1.71–1.85 (m, 2H). MS (ESI) m/z: 700 $(M+K)^+$

6.6.22. 1,1′-(Cyclohexane-1,4-diaminyl)bis(4-(2-fluorophenyl)-butane-1,2,4-trione) (3c)

Compound **3c** was prepared in a similar fashion as described for **1c**, as pale solid, yield 80.0%. ^{1}H NMR (400 MHz, $CDCl_3$): δ 15.50 (br, 2H); 7.98–7.94 (m, 2H); 7.57–7.52 (m, 2H); 7.30–7.21 (m, 2H); 7.20–7.15 (m, 2H); 7.05 (d, 2H, J = 8.1 Hz); 3.86 (m, 2H), 2.12 (m, 4H); 1.42–1.39 (m, 4H). EI-MS (m/z): 498 (M^+). HR-EIMS calcd for $C_{26}H_{24}N_2F_2O_6$: 498.1602, found: 498.1597. Analytical HPLC t_R = 26.12 min, 100% (solvent system A), t_R = 24.82 min, 100% (solvent system B).

6.6.23. 1,1′-(Cyclohexane-1,4-diaminyl)bis(4-(4-fluorophenyl)-butane-1,2,4-trione) (4c)

Compound **4c** was prepared in a similar fashion as described for **1c**, white solid, yield 70.0%. ^{1}H NMR (400 MHz, $CDCl_3$): δ 15.6 (br, 2H); 8.05–8.02 (m, 4H); 7.20–7.16 (m, 6H); 7.06 (d, 2H, J = 7.83 Hz); 3.92 (m, 2H); 2.13 (m, 4H); 1.46 (m, 4H). EI-MS (m/z): 498 (M^+). HR-EIMS calcd for $C_{26}H_{24}N_2F_2O_6$: 498.1602, found: 498.1630. Analytical HPLC t_R = 25.45 min, purity 99.3% (solvent system A); t_R = 22.54 min, purity 98.6% (solvent system B).

6.6.24. 4-(4-Fluorophenyl)-*N*-(1-(4-(4-fluorophenyl)-2,4-dioxobutanoyl)piperidin-4-yl)-2,4-dioxobutanamide

Compound **4d** was prepared in a similar fashion as described for **11d**. ^{1}H NMR (300 MHz, $CDCl_3$): δ 8.05–8.00 (m, 2H), 7.96–7.91 (m, 2H), 7.20–7.11 (m, 4H), 6.52 (s, 1H), 4.54 (m, 1H), 4.16–4.08 (m, 2H), 3.30–3.25 (m, 1H), 2.97–2.87 (m, 1H), 2.11–2.10 (m, 2H), 1.64–1.52 (m, 2H). MS m/z: 508.2 $(M)^+$. EI-MS (m/z, %): 388 (20.0); 165 (100.0); 138 (16.0); 123 (36.0). Analytical HPLC t_R = 26.05 min, purity 98.8% (solvent system A), t_R = 21.40 min, purity 98.6% (solvent system B).

6.6.25. 1,1′-(Piperazine-1,4-diyl)bis(4-(4-fluorophenyl)butane-1,2,4-trione)

Compound **4e** was prepared in a similar fashion as described for **1c**, pale yellow solid, yield 60.0%. ^{1}H NMR (400 MHz, $CDCl_3$): δ 7.97–7.92 (m, 4H); 7.20–7.14 (m, 4H); 6.61 (s, 2H); 3.78 (m, 8H). EI-MS (m/z, %): 470 (M^+, 7.0); 306 (5.0); 278 (14.0); 165 (43.0); 123 (100.0). HR-EIMS calcd for $C_{24}H_{20}N_2F_2O_6$: 470.1289, found: 470.1282. Analytical HPLC t_R = 24.86 min, purity 99.0% (solvent system A), t_R = 21.20 min, 100% (solvent system B).

6.6.26. 1,1′-(Cyclohexane-1,4-diaminyl)bis(4-(2-chlorophenyl) butane-1,2,4-trione) (9c)

Compound **9c** was prepared in a similar fashion as described for **1c**, white solid (113 mg, 85%). ^{1}H NMR (400 MHz, $CDCl_3$): δ 7.66 (d, 1H, J = 1.5 Hz), 7.65 (d, 1H, J = 1.4 Hz), 7.49–7.41 (m, 4H), 7.38–7.35 (m, 2H), 7.08 (s, 2H), 7.04 (d, 2H, J = 8.0 Hz), 3.86 (m, 2H), 2.13–2.11 (m, 4H), 1.49–1.41 (m, 4H). EI-MS (m/z): 530 (M^+-H); 532 (M^++H). HR-EIMS calcd for $C_{26}H_{24}N_2Cl_2O_6$: 530.1011, found: 530.0996. Analytical HPLC t_R = 26.95 min, purity 98.6% (solvent system A); t_R = 24.77 min, purity 97.9% (solvent system B).

6.6.27. 4-(2-Chlorophenyl)-*N*-{1-[4-(2-chlorophenyl)-2,4-dioxo-butyryl]-piperidin-4-yl}-2,4-dioxo-butyramide (9d)

Compound **9d** was prepared in a similar fashion as described for **11d**, red solid (85.7%). ^{1}H NMR (300 MHz, CD_3OD): δ 7.60–7.56 (m, 2H), 7.43–7.30 (m, 6H), 6.56 (s, 2H), 4.53–4.45 (m, 1H), 4.22–4.13 (m, 1H), 4.03–3.90 (m, 1H), 3.15–3.06 (m, 1H), 2.92–2.84 (m, 1H), 1.93–1.88 (m, 2H), 1.65–1.57 (m, 2H). ESI-MS m/z: 540.2 $(M+Na)^+$. Anal. ($C_{25}H_{22}Cl_2O_6N_2$) C 58.27, H 3.91, N 5.44. Found: C 58.05, H 3.73, N 5.63.

6.6.28. 1,1′-(Piperazine-1,4-diyl)bis(4-(2-chlorophenyl)butane-1,2,4-trione) (9e)

Compound **9e** was prepared in a similar fashion as described for **1c**, glassy solid (158 mg, 90%). ^{1}H NMR (400 MHz, $CDCl_3$): δ 7.70–7.67 (m, 2H); 7.49–7.36 (m, 6H); 6.57 (s, 2H); 3.87–3.76 (m, 8H). EI-MS (m/z): 502 (M^+-1). Analytical HPLC t_R = 25.99 min, purity 98% (solvent system A); t_R = 22.56 min, purity 95.0% (solvent system B).

6.6.29. 1,1′-(Cyclohexane-1,4-diaminyl)bis(4-(4-(trifluoromethyl) phenyl)butane-1,2,4-trione) (10c)

Compound **10c** was prepared in a similar fashion as described for **1c**, white solid, yield 90%. ^{1}H NMR (400 MHz, $CDCl_3$): δ 8.22 (m, 2H); 8.10 (m, 4H); 7.76 (m, 6H); 3.90 (m, 2H); 2.13 (m, 4H); 1.47 (m, 4H). EI-MS (m/z, %): 598 (M^+). HR-EIMS calcd for $C_{28}H_{24}N_2F_6O_6$: 598.1539, found: 598.1538. Analytical HPLC t_R = 30.24 min, purity 99.8% (solvent system A), t_R = 28.58 min, purity 99.6% (solvent system B).

6.6.30. 1,1′-(Piperazine-1,4-diyl)bis(4-(4-(trifluoromethyl)-phenyl)butane-1,2,4-trione) (10e)

Compound **10e** was prepared in a similar fashion as described for **1c**, white solid, yield 70%. ^{1}H NMR (400 MHz, $CDCl_3$): δ 8.03 (m, 4H), 7.75 (d, 4H, J = 7.9 Hz), 6.71 (s, 1H), 6.70 (s, 1H), 3.78 (m, 8H); EI-MS (m/z, %): 570 (M^+, 2.0); HR-EIMS Calcd. for $C_{26}H_{20}N_2F_6O_6$: 570.1226, found 570.1238. Analytical HPLC t_R = 25.96 min, purity 100% (solvent system A), t_R = 25.14 min, purity 100% (solvent system B).

6.6.31. 1,1′-(Cyclohexane-1,4-diaminyl)bis(4-(3-methoxy-phenyl)butane-1,2,4-trione) (11c)

Compound **11c** was prepared in a similar fashion as described for **1c**, white solid, yield 64.0%. ^{1}H NMR (400 MHz, $CDCl_3$): δ 7.59 (m, 2H); 7.50 (m, 2H); 7.40 (t, 2H, J = 8.0 Hz); 7.19 (s, 2H); 7.15–7.14 (m, 1H); 7.13–7.12 (m, 1H); 7.08 (d, 2H, J = 8.4 Hz); 3.87 (m, 2H), 3.87 (s, 6H), 2.12 (m, 4H); 1.50–1.42 (m, 4H). EI-MS (m/z): 522 (M^+). HR-EIMS calcd for $C_{28}H_{30}N_2O_8$: 522.2002, found: 522.2003. Analytical HPLC t_R = 27.75 min, purity 98.8% (solvent system A); t_R = 21.80 min, purity 100% (solvent system B).

6.6.32. 1,1′-(Piperazine-1,4-diyl)bis(4-(3-methoxyphenyl)-butane-1,2,4-trione) (11e)

Compound **11e** was prepared in a similar fashion as described for **1c**, white solid, yield 60.0%. ^{1}H NMR (400 MHz, $CDCl_3$): δ 7.51–7.36 (m, 6H); 7.13–7.11 (m, 2H); 6.63 (s, 2H); 3.85 (s, 6H); 3.78 (s, 8H). EI-MS (m/z): 494 (M^+). Analytical HPLC t_R = 25.87 min, purity 99.2% (solvent system A), t_R = 26.42 min, purity 100% (solvent system B).

Acknowledgments

National Natural Science Foundation of China (No. 30672528) and Science and Technology Commission of Shanghai Municipality (07QH14018) are greatly appreciated for the financial supports. The work in NN's laboratory was supported in part by funding from the Campbell Foundation.

References and notes

1. Agrawal, L.; Lu, X.; Jin, Q.; Alkhatib, G. *Curr. Pharm. Des.* **2006**, *12*, 2031.
2. Cohen, J. *Science* **2002**, *296*, 2320.
3. Asante-Appiah, E.; Skalka, A. M. *Antiviral Res.* **1997**, *36*, 139.
4. Bujacz, G.; Alexandratos, J.; Wlodawer, A. *J. Biol. Chem.* **1997**, *272*, 18161.
5. Yang, W.; Steitz, T. A. *Structure* **1995**, *3*, 131.
6. Grobler, J. A.; Stillmock, K.; Hu, B. H.; Witmer, M.; Felock, P.; Espeseth, A. S.; Wolfe, A.; Egbertson, M.; Bourgeois, M.; Melamed, J.; Wai, J. S.; Young, S.; Vacca, J.; Hazuda, D. J. *Proc. Natl. Acad. Sci. U.S.A.* **2002**, *99*, 6661.
7. Marchand, C.; Johnson, A. A.; Karki, R. G.; Pais, G. C. G.; Zhang, X. C.; Cowansage, K.; Patel, T. A.; Nicklaus, M. C.; Burke, T. R.; Pommier, Y. *Mol. Pharmacol.* **2003**, *64*, 600.
8. Pommier, Y.; Johnson, A. A.; Marchand, C. *Nat. Rev. Drug Disc.* **2005**, *4*, 236.
9. Pais, G. C. G.; Burke, T. R. *Drugs Future* **2002**, *27*, 1101.
10. Nair, V.; Chi, G. *Rev. Med. Virol.* **2007**, *17*, 277.
11. Hazuda, D. J.; Felock, P.; Witmer, M.; Wolfe, A.; Stillmock, K.; Grobler, J. A.; Espeseth, A.; Gabryelski, L.; Schleif, W.; Blau, C.; Miller, M. D. *Science* **2000**, *287*, 646.
12. Anthony, N.; Egbertson, M.; Melamed, J. Y.; Young, S.; Hamill, T.; Cole, J. L.; Hazuda, D. J. *Proc. Natl. Acad. Sci. U.S.A.* **2000**, *97*, 11244.
13. Marchand, C.; Zhang, X. C.; Pais, G. C. G.; Cowansage, K.; Neamati, N.; Burke, T. R.; Pommier, Y. *J. Biol. Chem.* **2002**, *277*, 12596.
14. (a) Dayam, R.; Al-Mawsawi, L. Q.; Neamati, N. *Drugs R&D* **2007**, *8*, 155; (b) Al-Mawsawi, L. Q.; Al-Safi, R. I.; Neamati, N. *Expert Opin. Emerg. Drugs* **2008**, *13*, 1.
15. Evering, T. H.; Markowitz, M. *Expert Opin. Invest. Drugs* **2008**, *17*, 413.
16. Goldgur, Y.; Craigie, R.; Cohen, G. H.; Fujiwara, T.; Yoshinaga, T.; Fujishita, T.; Sugimoto, H.; Endo, T.; Murai, H.; Davies, D. R. *Proc. Natl. Acad. Sci. U.S.A.* **1999**, *96*, 13040.
17. Long, Y.-Q.; Jiang, X.-H.; Dayam, R.; Sanchez, T.; Shoemaker, R.; Sei, S.; Neamati, N. *J. Med. Chem.* **2004**, *47*, 2561.
18. (a) Jiang, X.-H.; Song, L.-D.; Long, Y.-Q. *J. Org. Chem.* **2003**, *68*, 7555; (b) Jiang, X.-H.; Long, Y.-Q. *Chin. J. Chem.* **2004**, *22*, 978.
19. Wai, J. S.; Egbertson, M. S.; Payne, L. S.; Fisher, T. E.; Embrey, M. W.; Tran, L. O.; Melamed, J. Y.; Langford, H. M.; Guare, J. P., Jr.; Zhuang, L.; Grey, V. E.; Vacc, J. P.; Holloway, M. K.; Naylor-Olsen, A. M.; Hazuda, D. J.; Felock, P. J.; Wolfe, A. L.; Stillmock, K. A.; Schleif, W. A.; Gabryelski, L. J.; Young, S. D. *J. Med. Chem.* **2000**, *43*, 4923.
20. Pais, G. C. G.; Zhang, X. C.; Marchand, C.; Neamati, N.; Cowansage, K.; Svarovskaia, E. S.; Pathak, V. K.; Tang, Y.; Nicklaus, M.; Pommier, Y.; Burke, T. R. *J. Med. Chem.* **2002**, *45*, 3184.
21. GOLD 3.2, The Cambridge Crystallographic Data Centre, Cambridge, UK, 2005.
22. Catalyst, Accelrys, Inc., San Diego, USA.
23. Smellie, A.; Dyda, F.; Hickman, A. B. *J. Comput. Chem.* **1995**, *16*, 171.
24. Smellie, A.; Kahn, S. D.; Teig, S. L. *J. Chem. Inf. Comput. Sci.* **1995**, *35*, 285.
25. Smellie, A.; Kahn, S. D.; Teig, S. L. *J. Chem. Inf. Comput. Sci.* **1995**, *35*, 295.
26. Goldgur, Y.; Dyda, F.; Hickman, A. B.; Jenkins, T. M.; Craigie, R.; Davies, D. R. *Proc. Natl. Acad. Sci. U.S.A.* **1998**, *95*, 9150.
27. Verdonk, M. L.; Chessari, G.; Cole, J. C.; Hartshorn, M. J.; Murray, C. W.; Nissink, J. W.; Taylor, R. D.; Taylor, R. *J. Med. Chem.* **2005**, *48*, 6504.
28. Verdonk, M. L.; Cole, J. C.; Hartshorn, M. J.; Murray, C. W.; Taylor, R. D. *Proteins* **2003**, *52*, 609.